**Supporting Information for**

# Direct Ink Writing of Polyimide Aerogels for Battery Thermal Mitigation

Ciera E. Cipriani,[1] Donald A. Dornbusch,[2] Stephanie L. Vivod,[2*] Emily B. Pentzer*[1,3]

[1]Department of Materials Science and Engineering, Texas A&M University, 3003 TAMU, College Station, Texas 77843, United States
[2]NASA Glenn Research Center, 21000 Brookpark Road, Cleveland, Ohio 44135, United States
[3]Department of Chemistry, Texas A&M University, 3255 TAMU, College Station, Texas 77843, United States

*Email: emilypentzer@tamu.edu

**Table S1.** Dimensions, linear shrinkage values, masses, and densities of cast and printed compression cylinders.

| | Height (mm) | Diameter (mm) | Linear Shrinkage (%) | Mass (g) | Density (g/cm³) |
|---|---|---|---|---|---|
| | 15.42 | 12.48 | 12.30 | 0.206 | 0.109 |
| | 11.34 | 12.54 | 11.88 | 0.153 | 0.109 |
| **Cast** | 14.9 | 12.55 | 11.81 | 0.200 | 0.109 |
| | 11.28 | 12.55 | 11.81 | 0.152 | 0.109 |
| | 12.48 | 12.54 | 11.88 | 0.167 | 0.108 |
| | 10.46 | 11.85 | 16.67 | 0.120 | 0.093 |
| | 10.34 | 11.43 | 19.67 | 0.118 | 0.100 |
| **Printed** | 8.56 | 12.45 | 12.53 | 0.123 | 0.103 |
| | 10.87 | 12.68 | 10.87 | 0.154 | 0.105 |
| | 10.28 | 12.41 | 12.80 | 0.124 | 0.100 |

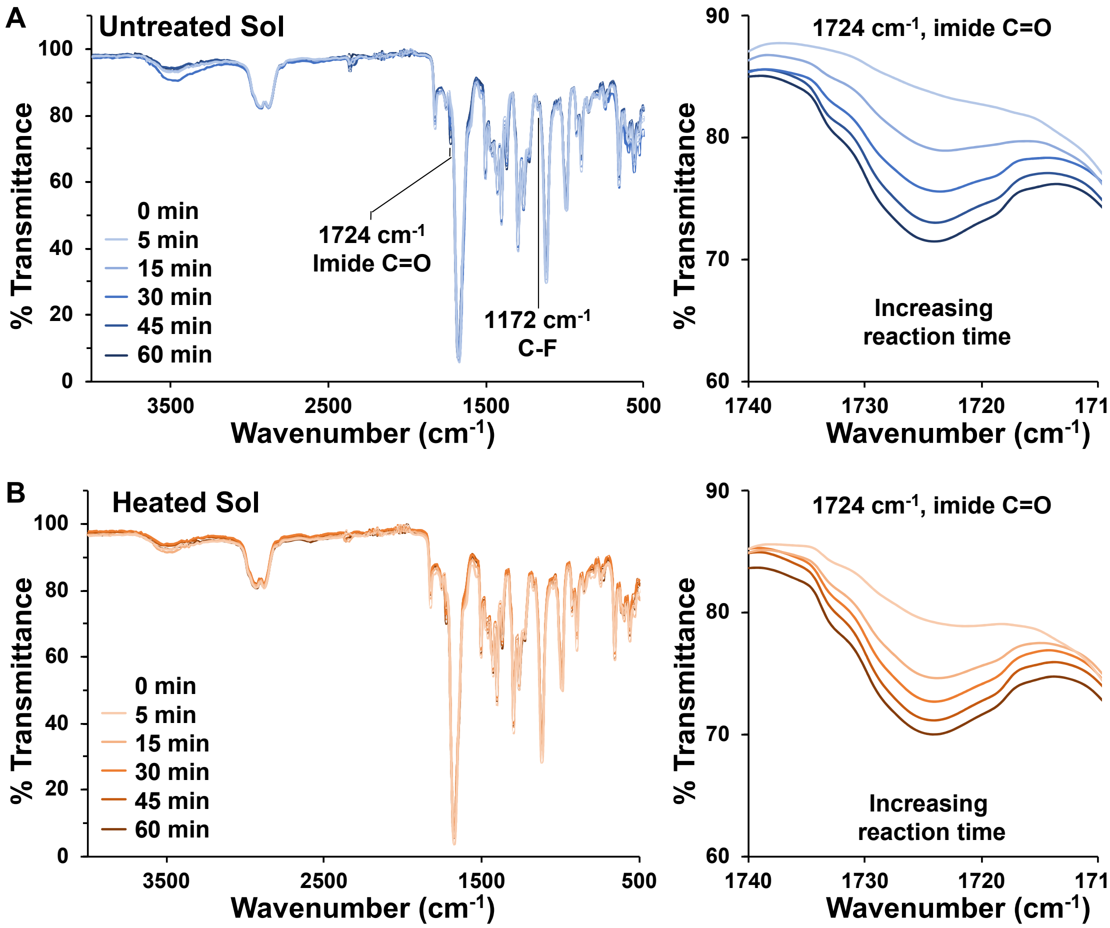


**Figure S1.** FTIR spectra during various timepoints after addition of TEA catalyst, normalized at 1172 $cm^{-1}$. (A, left) Untreated sol, showing peaks corresponding to imide C=O at 1724 $cm^{-1}$ and C-F at 1172 $cm^{-1}$. (A, right) Expansion of imide C=O region indicating increasing transmittance with increasing reaction time in untreated sol. (B, left) Heated sol. (B, right) Expansion of imide C=O region indicating increasing transmittance with increasing reaction time in heated sol.

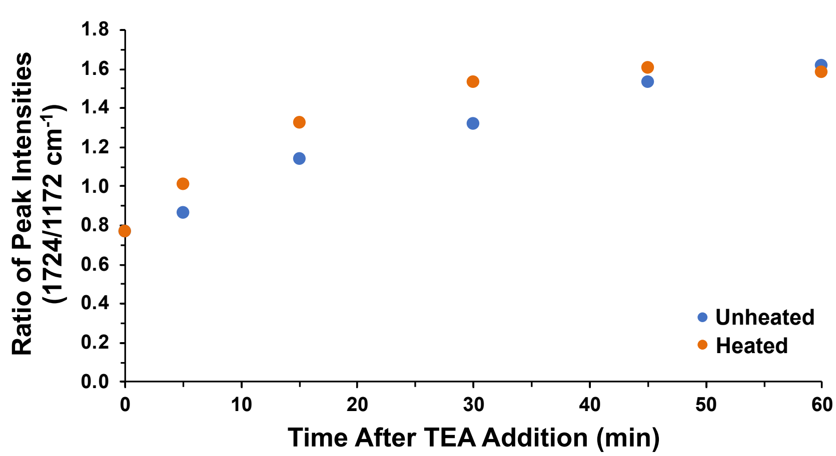


**Figure S2.** Ratios of intensities of C=O and C-F peaks in FTIR spectra over reaction time.

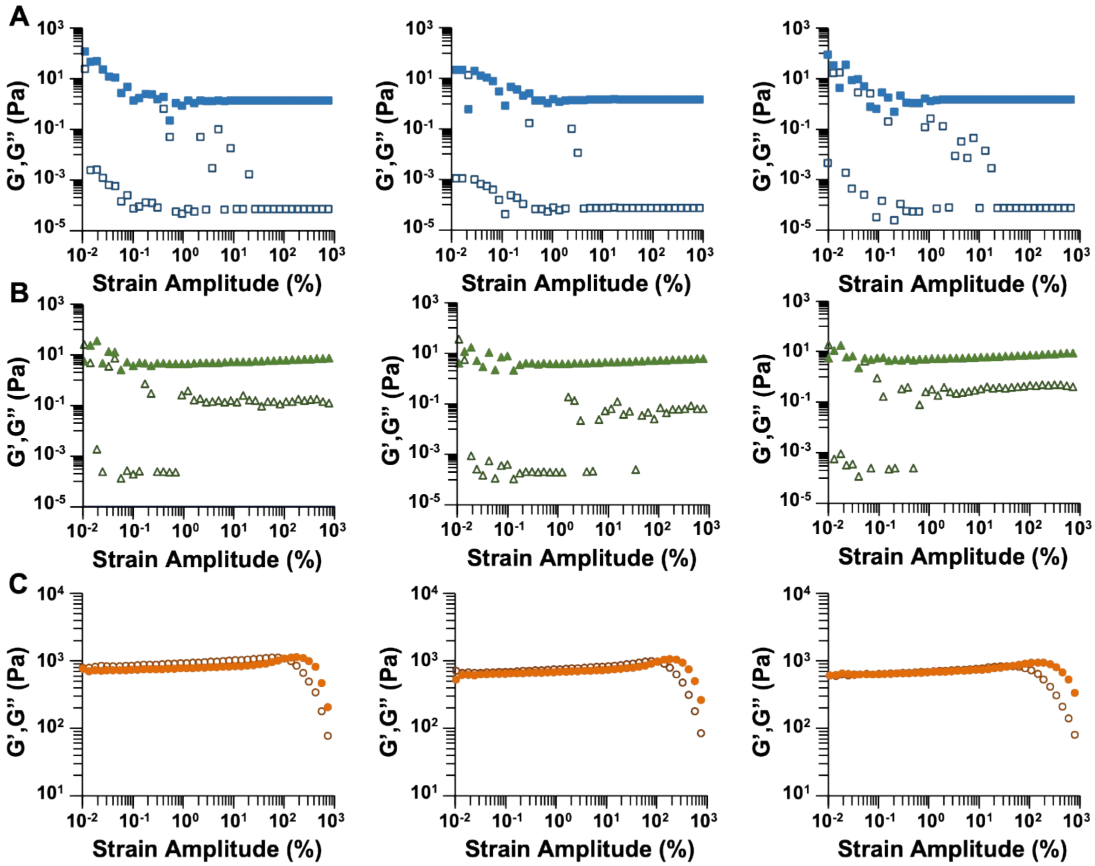


**Figure S3.** G' and G" as a function of strain amplitude for three samples of (A) untreated sol, (B) aged sol, (C) ink.

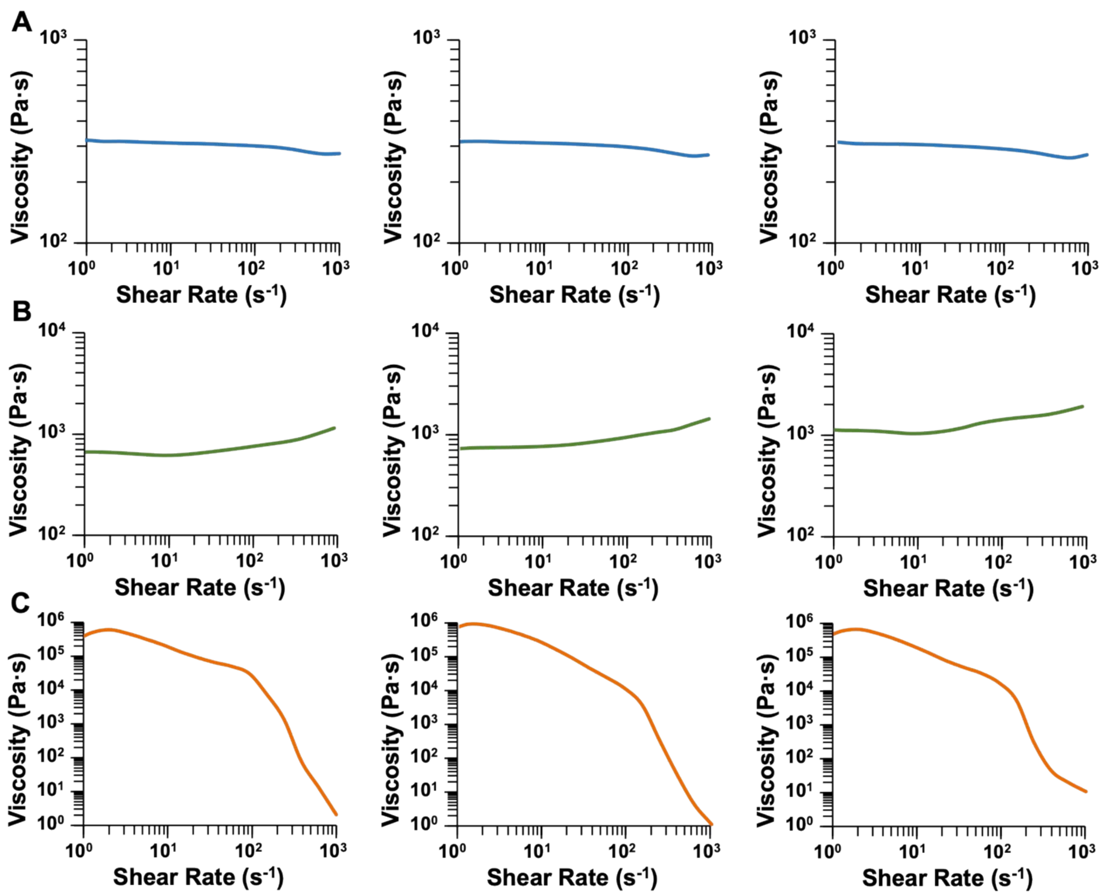


**Figure S4.** Viscosity as a function of shear rate for three samples of (A) untreated sol, (B) aged sol, (C) ink.

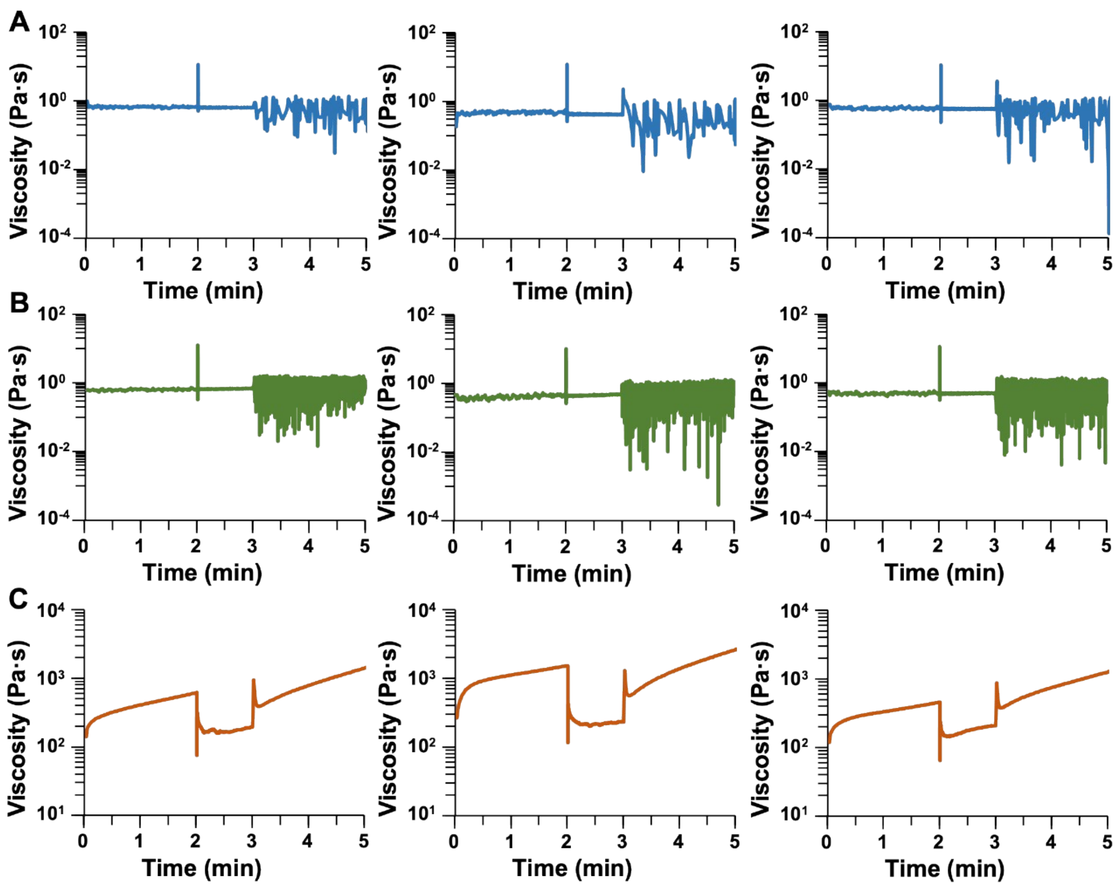


**Figure S5.** Viscosity as a function of time during the 3ITT for three samples of (A) untreated sol, (B) aged sol, (C) ink.

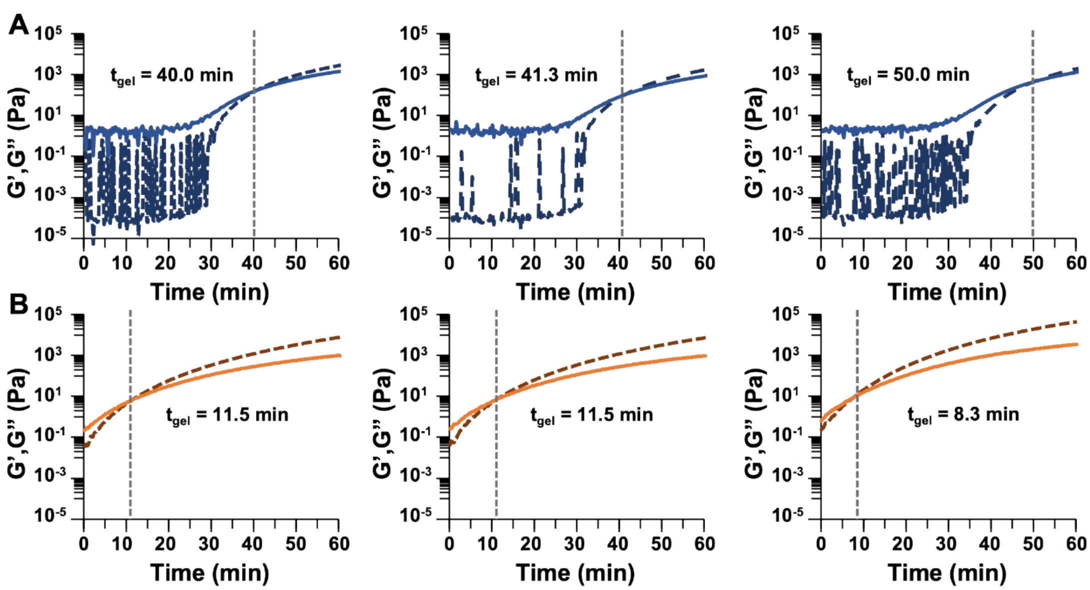


**Figure S6.** G' and G" as a function of time and gel points for three samples of (A) untreated sol and (B) ink.

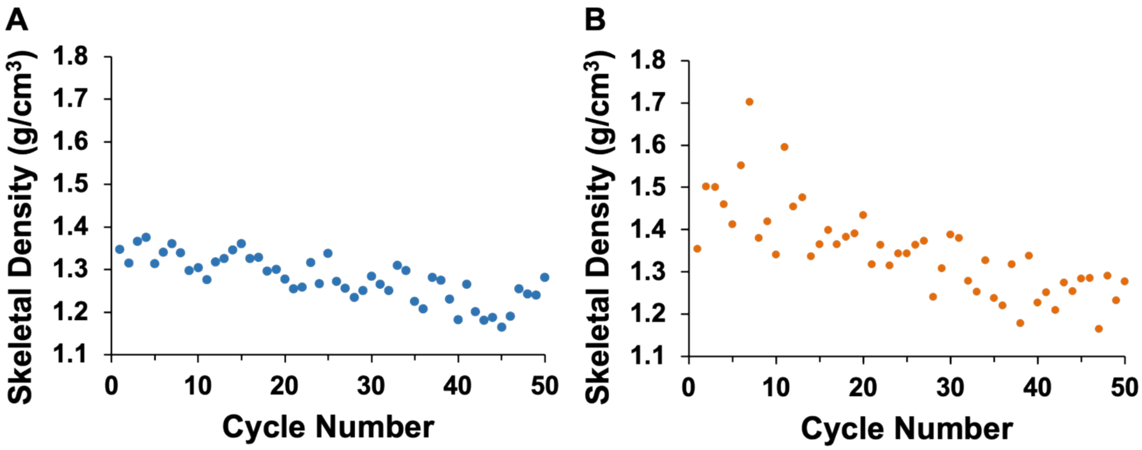


**Figure S7.** Skeletal density of (A) cast aerogel and (B) printed aerogel throughout 50 chamber filling cycles.

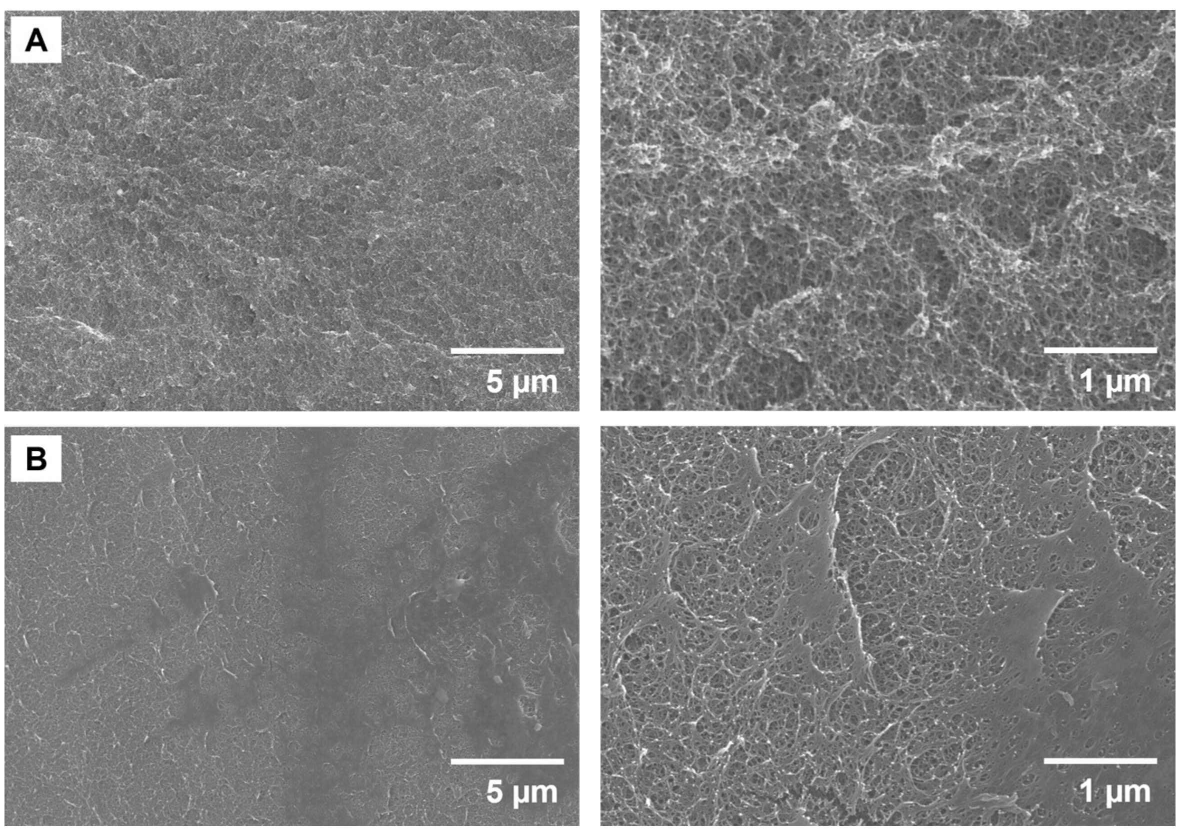


**Figure S8.** Scanning electron micrographs of fractured surfaces of (A) cast aerogel and (B) printed aerogel.

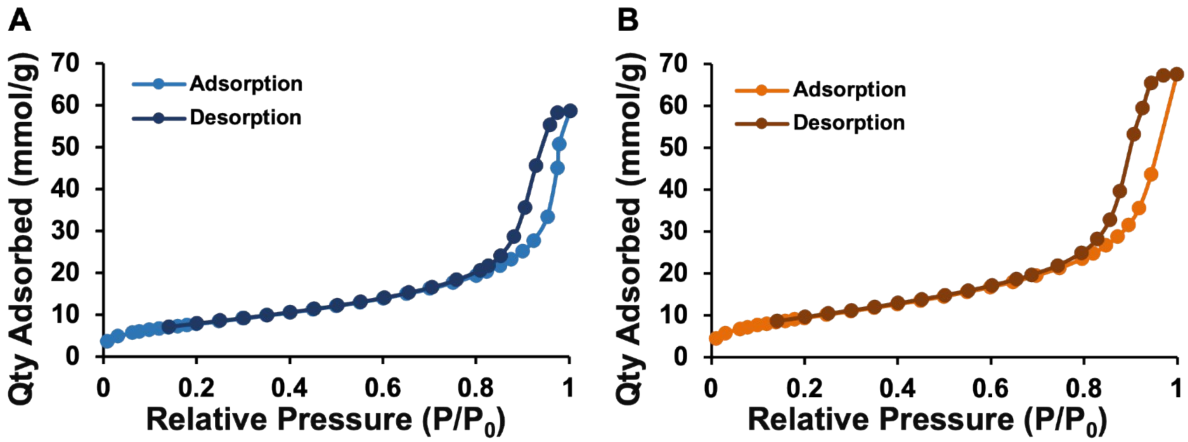


**Figure S9.** Adsorption-desorption curves of nitrogen onto (A) cast aerogel and (B) printed aerogel.

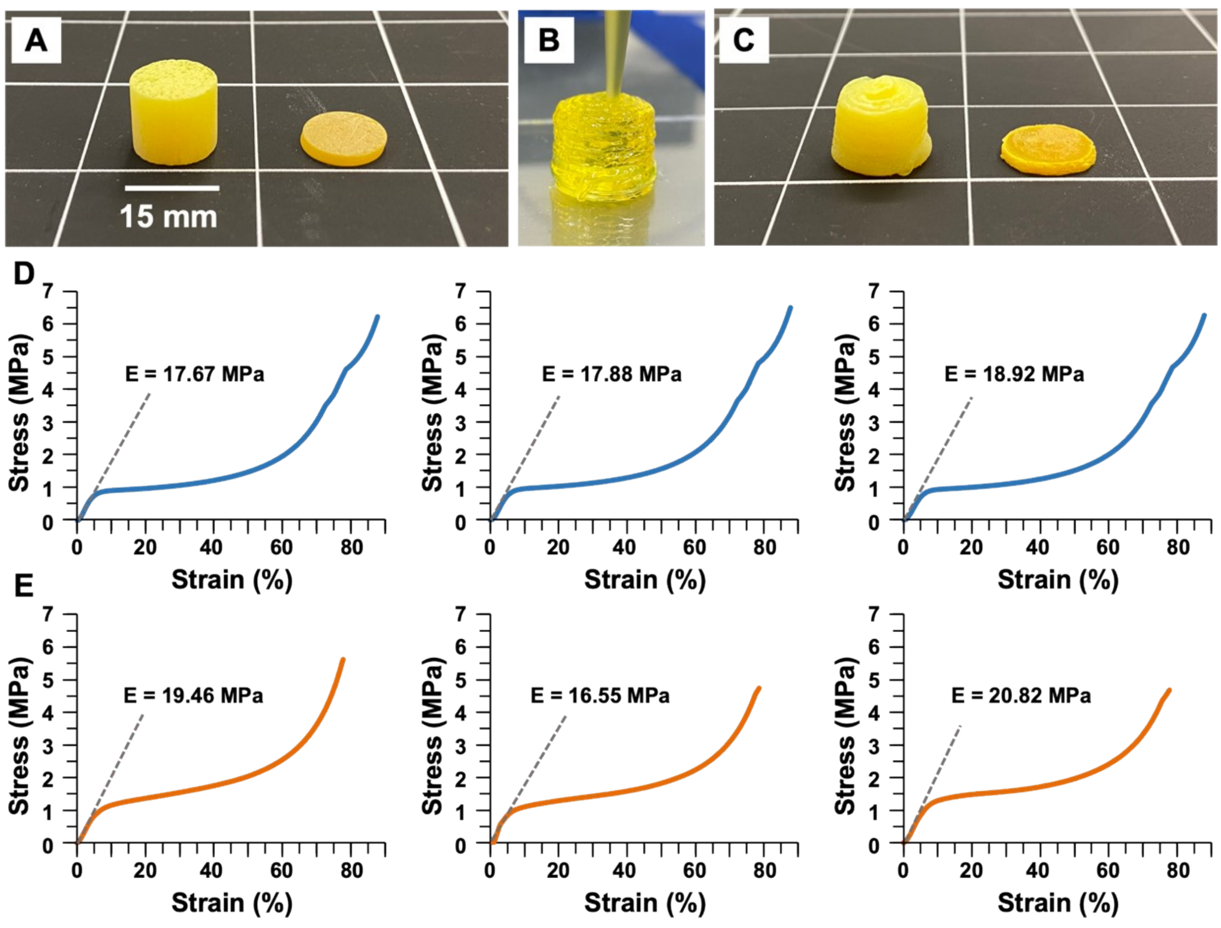


**Figure S10.** Compression test data. (A) Cast compression cylinder before (left) and after (right) testing. (B) DIW of compression cylinder. (C) Printed compression cylinder before (left) and after (right) testing. (D) Stress-strain profiles of three samples of cast aerogel. (E) Stress-strain profiles of three samples of printed aerogel.

**Table S2.** Thermal conductivities of cast and printed aerogels at various temperatures.

| | Thermal Conductivity (mW/m K) | | | | | |
|---|---|---|---|---|---|---|
| **Temperature (°C)** | **Cast Aerogel** | | | **Printed Aerogel** | | |
| **-50** | 39.6 | 39.3 | 39.4 | 24.0 | 24.4 | 23.4 |
| **-25** | 38.9 | 39.7 | 40.5 | 27.1 | 26.3 | 27.3 |
| **0** | 39.1 | 39.6 | 39.6 | 30.7 | 30.8 | 30.6 |
| **25** | 37.8 | 41.7 | 40.6 | 37.2 | 38.5 | 37.6 |
| **50** | 34.4 | 34.6 | 34.5 | 35.2 | 34.5 | 34.7 |
| **75** | 32.4 | 32.9 | 32.7 | 36.9 | 36.2 | 37.1 |
| **100** | 33.4 | 32.5 | 33.6 | 38.3 | 37.5 | 37.9 |
| **125** | 36.5 | 37.0 | 36.4 | 42.9 | 41.6 | 42.4 |
| **150** | 39.5 | 40.3 | 39.2 | 42.8 | 42.8 | 43.8 |

**Table S3.** Surface temperatures of heating plate and aerogel throughout thermal insulation experiment. Each row corresponds to one temperature setting, and three measurements were taken on each surface at each setting 5 min after the plate temperature equilibrated.

| **Heating Plate Temperature (°C)** | | | **Aerogel Temperature (°C)** | | |
|---|---|---|---|---|---|
| 43.0 | 42.2 | 42.6 | 24.6 | 24.4 | 24.6 |
| 51.6 | 53.6 | 50.0 | 25.4 | 26.2 | 25.0 |
| 81.9 | 82.9 | 84.0 | 26.0 | 26.4 | 25.7 |
| 105.8 | 111.9 | 112.8 | 26.4 | 26.4 | 25.3 |
| 121.7 | 117.4 | 123.0 | 27.4 | 26.6 | 25.9 |

**Table S4.** Surface temperatures of heating plate and aerogel over time at maximum heating plate temperature (approximately 120 °C).

| **Time (min)** | **Heating Plate Temperature (°C)** | | | **Aerogel Temperature (°C)** | | |
|---|---|---|---|---|---|---|
| 5 | 121.7 | 117.4 | 123.0 | 27.4 | 26.6 | 25.9 |
| 30 | 119.8 | 121.2 | 120.9 | 28.8 | 29.2 | 30.0 |
| 60 | 120.1 | 120.4 | 118.9 | 29.3 | 30.9 | 30.0 |
| 90 | 118.8 | 119.6 | 120.8 | 30.1 | 30.9 | 29.4 |
| 120 | 119.1 | 119.2 | 120.5 | 30.0 | 28.9 | 29.7 |